Development 137, 2147-2156 (2010) doi:10.1242/dev.037150


# CARM1 is required for proper control of proliferation and differentiation of pulmonary epithelial cells

**Karen B. O'Brien[1], Meritxell Alberich-Jordà[1], Neelu Yadav[2], Olivier Kocher[3], Annalisa DiRuscio[1], Alexander Ebralidze[1], Elena Levantini[3], Natasha J. L. Sng[3], Manoj Bhasin[3], Tyler Caron[4], Daehoon Kim[5], Ulrich Steidl[6], Gang Huang[7], Balázs Halmos[8], Scott J. Rodig[4], Mark T. Bedford[5], Daniel G. Tenen[1,9,*] and Susumu Kobayashi[3,*]**

## SUMMARY

Coactivator-associated arginine methyltransferase I (CARM1; PRMT4) regulates gene expression by multiple mechanisms including methylation of histones and coactivation of steroid receptor transcription. Mice lacking CARM1 are small, fail to breathe and die shortly after birth, demonstrating the crucial role of CARM1 in development. In adults, CARM1 is overexpressed in human grade-III breast tumors and prostate adenocarcinomas, and knockdown of CARM1 inhibits proliferation of breast and prostate cancer cell lines. Based on these observations, we hypothesized that loss of CARM1 in mouse embryos would inhibit pulmonary cell proliferation, resulting in respiratory distress. By contrast, we report here that loss of CARM1 results in hyperproliferation of pulmonary epithelial cells during embryonic development. The lungs of newborn mice lacking CARM1 have substantially reduced airspace compared with their wild-type littermates. In the absence of CARM1, alveolar type II cells show increased proliferation. Electron microscopic analyses demonstrate that lungs from mice lacking CARM1 have immature alveolar type II cells and an absence of alveolar type I cells. Gene expression analysis reveals a dysregulation of cell cycle genes and markers of differentiation in the *Carm1* knockout lung. Furthermore, there is an overlap in gene expression in the *Carm1* knockout and the glucocorticoid receptor knockout lung, suggesting that hyperproliferation and lack of maturation of the alveolar cells are at least in part caused by attenuation of glucocorticoid-mediated signaling. These results demonstrate for the first time that CARM1 inhibits pulmonary cell proliferation and is required for proper differentiation of alveolar cells.

**KEY WORDS: CARM1 (PRMT4), Mouse, Gene deletion, Cell differentiation, Cell proliferation, Lung pathology, Gene expression profiling, Pulmonary cell, Alveolar, Respiratory development, Respiratory distress, BASC**

## INTRODUCTION

Coactivator-associated arginine methyltransferase I [CARM1; also known as protein arginine methyltransferase 4 (PRMT4)] is one of nine members of the protein arginine methyltransferase (PRMT) family that regulate crucial cellular functions, including transcription, mRNA processing and stability, and translation. CARM1 positively regulates transcription by methylating histone H3 at arginine 17 and 26 and therefore belongs to a crucial group of regulatory factors that dynamically shape the nuclear environment and specify transcriptional states (Bedford and Richard, 2005; Cook et al., 2006). CARM1 is a transcriptional coactivator of nuclear receptors and methylates steroid receptor coactivators [SRC3 (NCOA3) and CBP/p300 (CREBBP)]. Methylation of these proteins increases steroid receptor transcription (Bauer et al., 2002; Chevillard-Briet et al., 2002; Daujat et al., 2002; Feng et al., 2006; Ma et al., 2001; Schurter et al., 2001; Xu et al., 2001). CARM1 also increases the transcriptional activity of other factors, including cFOS, p53 (TRP53), NFκB and LEF1/TCF4 (An et al., 2004; Covic et al., 2005; Fauquier et al., 2008; Koh et al., 2002; Miao et al., 2006; Teyssier et al., 2006; Yang et al., 2006). Furthermore, CARM1 methylates the RNA-binding proteins HuR and HuD (ELAVL1 and ELAVL4), modulating their ability to bind and stabilize transcripts (Fujiwara et al., 2006; Li et al., 2002; Yamaguchi et al., 1994). Lastly, CARM1 methylates splicing factors such as CA150 (TCERG1) to regulate exon skipping (Cheng et al., 2007; Mastrianni et al., 1992; Yadav et al., 2003).

CARM1 has also been implicated in cancer cell proliferation. CARM1 is overexpressed in grade-III breast cancers (El Messaoudi et al., 2006; Frietze et al., 2008) and in prostate adenocarcinomas (Hong et al., 2004; Majumder et al., 2006). In estrogen-treated MCF-7 human breast cancer cells, CARM1 knockdown results in reduced cellular proliferation and cell cycle progression. CARM1 localizes to the promoters and positively regulates the expression of E2F1 and cyclin E1, factors that increase cell cycle progression (El Messaoudi et al., 2006; Frietze et al., 2008). Similarly, knockdown of CARM1 inhibits prostate cell growth both in the presence and absence of androgen stimulation and induces apoptosis (Majumder et al., 2006). Taken together, these observations indicate that CARM1 regulates cell cycle progression and cellular growth in response to steroids. Given these functions, it is not surprising that CARM1 plays a crucial role in

[1]Harvard Stem Cell Institute and Center for Life Sciences, Harvard Medical School, Boston, MA 02115, USA. [2]Department of Biological Sciences, State University of New York at Buffalo, Buffalo, NY 14260, USA. [3]Beth Israel Deaconess Medical Center, Boston, MA 02215, USA. [4]Department of Pathology, Brigham and Women's Hospital, Boston, MA 02115, USA. [5]The University of Texas, M.D. Anderson Cancer Center, Science Park, Smithville, TX 78957, USA. [6]Albert Einstein College of Medicine, Bronx, NY 10461, USA. [7]Cincinnati Children's Hospital Medical Center, Cincinnati, OH 45229, USA. [8]Herbert Irving Comprehensive Cancer Center, Columbia University Medical Center, New York, NY 10032, USA. [9]Cancer Sciences Institute, National University of Singapore, 117456 Singapore.

*Authors for correspondence (dtenen@bidmc.harvard.edu; skobayas@bidmc.harvard.edu)

**Accepted 17 April 2010**

development. Mice with a targeted deletion of *Carm1* (*Carm1*$^{\Delta/\Delta}$) are small and have defects in the differentiation of multiple cell types including T cells and adipocytes (Kim et al., 2004; Yadav et al., 2008; Yadav et al., 2003). Recently, it has been shown that mice carrying the enzyme-dead form of CARM1 phenocopy the *Carm1* knockout, suggesting that CARM1 requires enzymatic activity for its known cellular functions (Kim et al., 2009). *Carm1* knockout animals die shortly after birth and suffer from respiratory distress. *Carm1*$^{\Delta/\Delta}$ animals fail to inflate their lungs after birth, and have reduced alveolar air space compared with wild-type littermates. These observations suggest that CARM1 is an important regulator of lung development. However, detailed studies of CARM1 expression and function in lung have not been described.

Development of the distal lung and alveolar sacculation are tightly regulated by a myriad of hormone signals and a cascade of interacting transcription factor pathways that are just beginning to be elucidated (Cardoso and Lu, 2006; Maeda et al., 2007). Progenitor cells in the distal lung differentiate to multiple types including Clara bronchiole epithelial cells and alveolar type II (AT2) cells. AT2 cells are cuboidal and located in the alveolar sacs that produce the surfactant required to reduce surface tension for these sacs to fill with air. AT2 cells differentiate to alveolar type I (AT1) epithelial cells that coordinate air exchange to capillaries in the distal lung. Given that CARM1 functions to enhance the growth and proliferation of breast and prostate cancer cells, we hypothesized that the reduced airspace seen in *Carm1*$^{\Delta/\Delta}$ lungs results from inhibited alveolar cell proliferation, resulting in loss of surfactant protein and collapsed alveolar sacs.

In this study, we demonstrate that CARM1 is expressed in pulmonary epithelial cells. Contrary to our expectation that loss of CARM1 would result in reduced cellular growth, we observed hyperproliferation of AT2 cells in the lung of *Carm1*$^{\Delta/\Delta}$ mice. We further demonstrate a block in differentiation from AT2 to AT1 cells in the absence of CARM1. Microarray analysis reveals a loss of expression of genes crucial for cell cycle regulation and AT1 differentiation. Together, these data demonstrate for the first time that CARM1 is expressed in the lung and is crucial for development, growth and pulmonary epithelial cell function. The data further demonstrate that pulmonary cell proliferation increases in the absence of CARM1, in direct contrast to findings in other tissues.

## MATERIALS AND METHODS

### Mouse generation and genotyping

The generation of mice with targeted disruption of *Carm1* (*Carm1*$^{\Delta/\Delta}$ mice) has been described (Yadav et al., 2003). The targeting strategy resulted in a disruption of transcription at exon 2, and a predicted null phenotype that was confirmed by immunofluorescence and western blot analysis. The genotyping of *Carm1*$^{\Delta/\Delta}$ mice has been described previously (Yadav et al., 2003).

### Antibodies and immunohistochemistry (IHC)

Lung tissues were fixed in 10% paraformaldehyde overnight at 4°C. The following antibodies and dilutions were used for IHC: anti-CARM1 (1:1000; IHC-00045, Bethyl Laboratories); anti-SPC (1:1000; SC-7705, Santa Cruz Biotechnology); anti-CCSP (1:1000; SC-9772, Santa Cruz Biotechnology); anti-AQP5 (1:500; ab78486, Abcam); anti-Ki-67 (1:250; clone SP6, Vector Laboratories); and anti-vWF (1:1000; A0082, DAKO). Fixed, paraffin-embedded tissue sections were deparaffinized and endogenous peroxidase activity was quenched in 1% phosphate-buffered $H_2O_2$ for 15 minutes at room temperature. Antigen retrieval was achieved by steaming slides in 10 mM citric acid (anti-CARM1, -SPC) or EDTA (anti-CCSP, -AQP5, -Ki-67, -vWF). Antibody staining was detected using the appropriate mouse or rabbit Envision Kit (DAKO) with DAB and counterstained with Hematoxylin according to standard protocols. For the double-marker IHC, slides were incubated with normal horse serum blocking solution for 30 minutes. Subsequently, the slides were incubated with the first primary antibody for 1 hour (anti-SPC, -CCSP or -vWF) using a similar DAB detection system as described above for the single-marker IHC. Then, slides were incubated with the second primary antibody (anti-CARM1 and -Ki-67) for 1 hour, followed by detection with the alkaline phosphatase-Fast Red system.

### Transmission electron microscopy (TEM)

Embryonic lungs were isolated, dissected to 0.5 cm cubes and placed in fixing buffer (2.5% glutaraldehyde in 0.1 M sodium cacodylate buffer) overnight at 4°C and subsequently stored at 4°C in 0.1 M sodium cacodylate buffer. The samples were subsequently dehydrated in ascending alcohols, cleared with propylene oxide, and infiltrated with a mixture of Epon resin and propylene oxide overnight. They were then infiltrated with pure Epon resin and polymerized at 60°C for 48 hours. The hardened blocks were sectioned at 70 nm on a Reichert-Jung Ultracut E ultramicrotome. The sections were placed on nickel grids and stained for contrast with uranyl acetate and lead citrate. They were viewed and photographed on a JEOL JEM-1011 electron microscope.

### Quantitative real-time (qRT) PCR analysis

qRT-PCR analysis was performed in a Rotor Gene 6000 Sequence Detection System (Corbett Life Science). RNA was isolated, DNase I treated, reverse transcribed, and ~10 ng of the resulting cDNA was used in amplification reactions with SYBR Green PCR Master Mix (Applied Biosystems) and 500 nM of each gene-specific forward or reverse primer (see Table S1 in the supplementary material). For each gene, at least four wild-type and three *Carm1*$^{\Delta/\Delta}$ littermates were tested. qRT-PCR reactions consisted of one cycle of 95°C for 10 minutes, followed by 40 cycles of 95°C for 20 seconds and 60°C for 1 minute.

### Western blot analysis

Twenty-five micrograms of total lung protein were separated by SDS-PAGE, transferred to nitrocellulose and blocked in 5% non-fat milk. Proteins were immunoblotted with rabbit polyclonal anti-CARM1 (1:2000; ab51742, Abcam), which detects a region that is predicted to be deleted in the targeted allele.

### Flow cytometry and isolation of RNA from sorted populations

Pulmonary cells from 12-week-old mice were isolated as described (Kim et al., 2005). Sca-1-FITC, CD45.1- and CD45.2-biotin, pecam1-biotin, and streptavidin-TC were from BD Pharmingen and viable cells were isolated based on the exclusion of propidium iodide. Cell sorting was performed with a high-speed cell sorter (MoFlo, Beckman Coulter). Cells were collected in RLT buffer containing 1% β-mercaptoethanol and 20 ng bacterial carrier RNA (Roche Diagnostics) per sample according to the RNeasy Micro protocol (Qiagen) optimized for small amounts of RNA. RNA was then reverse transcribed and subjected to qRT-PCR analysis.

### Chromatin immunoprecipitation (ChIP) assay

Cross-linking, nuclei isolation and ChIP assay were performed as previously described (Ebralidze et al., 2008). Briefly, lung cells from E18.5 wild-type mice were cross-linked with 1% formaldehyde for 10 minutes at room temperature and nuclei were collected as follows. Approximately $1\times10^6$ cells were washed three times with ice-cold PBS supplemented with 1 mM PMSF. The cell pellet was resuspended in lysis buffer [10 mM Tris-HCl pH 8.0, 10 mM NaCl, 0.5% NP40, freshly supplemented with protease inhibitors (Roche Applied Science)], homogenized, and incubated for 15 minutes on ice. Nuclei were recovered by centrifugation at 600 ***g*** for 10 minutes, resuspended in 500 μl of storage buffer (1.75 ml water, 2 ml glycerol, 0.2 ml 20× Buffer A) supplemented with protease inhibitors, and stored at –80°C. ChIP was performed using the ChIP-IT Kit according to the manufacturer's recommendations (Active Motif) using antibodies to CARM1 (ab51742, Abcam), p53 (sc-6243, Santa Cruz) and glucocorticoid receptor (ab3579, Abcam) and rabbit IgG (53007, Active Motif). Primers used for *Scn3b* were 5′-CTAGAGAACAGGAGAAAAGGGCCT-3′ and 5′-CGAGCTTCGGATAAGCTTTAGGGT-3′. Promoter analysis was performed with MatInspector V2.2 software (Quandt et al., 1995).

### RNA interference

*Carm1*-specific (ON-TARGET plus SMART pool) and non-targeting control (ON-TARGET plus Non-Target) small interfering RNAs (siRNA) were purchased from Dharmacon. BEAS-2B cells were transfected using DharmaFECT transfection reagents (Dharmacon) according to the manufacturer's protocol. At 48 hours post-transfection, cells were incubated with RPMI containing 10% FBS in the presence of 0.1% ethanol (control) or 500 nM dexamethasone (Sigma-Aldrich) for an additional 72 hours. RNA isolation and qRT-PCR analysis were performed as described above.

### Statistical analysis

The paired Student's *t*-test was used to determine statistical significance.

## RESULTS

### CARM1 is expressed in alveolar type II, Clara epithelial and endothelial cells

Since we observed respiratory distress and reduced airspace in the distal lung of $Carm1^{\Delta/\Delta}$ mice, we first asked which pulmonary cells express CARM1. We stained lung tissue from E18.5 mouse embryos and observed CARM1 expression throughout the lung but not in all cells (Fig. 1A). CARM1 was found predominantly in the nucleus, with some cytoplasmic staining (Fig. 1B), and expression was high in cuboidal alveolar cells and in cells lining the terminal bronchioles (Fig. 1B). As expected, no CARM1 staining was detected in lungs from $Carm1^{\Delta/\Delta}$ mice (Fig. 1C). To determine whether CARM1 expression is limited to embryogenesis, we stained lung tissue from adult mice with anti-CARM1 and observed a similar expression pattern to that in embryonic lungs (Fig. 1D). In the adult lung, CARM1 was expressed in both the nucleus and cytoplasm, primarily in rounded epithelial cells (Fig. 1E).

To identify which cells express CARM1, we performed double staining of CARM1 with surfactant-associated protein C (SPC; SFTPC – Mouse Genome Informatics), which is expressed by AT2 cells. As expected, we observed cytoplasmic staining of SPC throughout the lung, particularly in rounded cells between air spaces and near the bronchial termini (Fig. 2A, brown stain). When SPC staining was combined with that of CARM1 (Fig. 2A, pink stain), we observed substantial overlap, indicating that CARM1 is expressed in SPC-positive AT2 cells (Fig. 2A, arrows). In addition to cuboidal cells, we observed CARM1 staining in cells surrounding the terminal bronchi. Thus, we examined whether CARM1 is expressed in the CCSP-positive Clara epithelial cells that line airways. CCSP (SCGB1A1 – Mouse Genome Informatics), a crucial secretory protein produced by Clara cells, was observed exclusively in the cells lining the bronchial airways of the embryonic lung (Fig. 2B, brown). When combined with anti-CARM1 (Fig. 2B, pink), we observed CCSP staining in the cytoplasm (brown) and CARM1 staining predominantly in the nuclei (pink), indicating that CARM1 is expressed in Clara cells (Fig. 2B). In addition, we observed co-expression of von Willebrand factor (vWF) and CARM1 (see Fig. S1 in the supplementary material), demonstrating that CARM1 is expressed in endothelial cells.

It has been proposed that AT2 and Clara cells are differentiated from bronchioalveolar stem cells (BASCs), which are located at the bronchioalveolar junction and are double positive for SPC and CCSP (Kim et al., 2005). To determine whether CARM1 is expressed in BACS, we isolated BASCs and AT2 cells by flow cytometry and measured *Carm1* expression in these populations by qRT-PCR. Fig. 2C is a representative sorting analysis from 8- to 12-week-old mice. We observed that

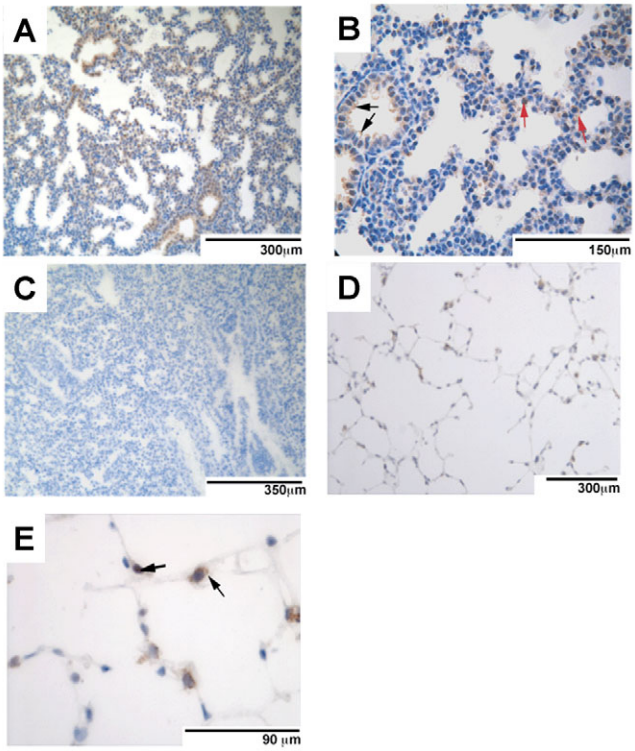


**Fig. 1. Immunohistochemical analysis of CARM1 in embryonic and adult murine lung.** (**A-E**) Lung sections from E18.5 (A-C) and 12-week-old (D,E) mice were stained with anti-CARM1. (A) Staining of CARM1 is observed throughout the embryonic lung. (B) High-magnification image showing that CARM1 is expressed in both the nucleus (left red arrow) and cytoplasm (right red arrow) of cuboidal AT2 cells in the spaces between alveolar sacs as well as in epithelial cells lining the terminal bronchioles (black arrows). (C) CARM1 staining is absent in mice with a targeted deletion of *Carm1*. (D,E) CARM1 expression is observed in cuboidal AT2 cells (D) and in the nucleus (E, left arrow) and cytoplasm (E, right arrow) of adult lung cells.

the BASC population constituted 0.3-0.8% of total lung cells from each animal, whereas the AT2 population ranged from 5 to 10%. As shown in Fig. 2D, *Carm1* mRNA was expressed in whole lung and in AT2 and BASCs. *Carm1* expression in whole lung constituted 0.48-1.5% of that of *Gapdh*, reflecting the multiple cell types observed by IHC (Fig. 1). *Carm1* expression in AT2 cells was consistent between animals at 0.8-1.2% of *Gapdh*. These data support the IHC data demonstrating CARM1 protein in AT2 cells. Since the BASC population is so small, we pooled isolated BASCs from two and three animals to obtain enough RNA to accurately measure *Carm1* expression. We observed *Carm1* expression in BASCs at 0.25% and 0.5% of *Gapdh*, respectively, in each of the pooled populations, demonstrating that *Carm1* expression in AT2 cells was 67% higher than in BASCs ($P$=0.02; Fig. 2D).

### Loss of CARM1 leads to hyperproliferation of pulmonary cells

We next sought to identify the role of CARM1 in pulmonary development. $Carm1^{\Delta/\Delta}$ mouse embryos survive to birth and respond to stimulus but suffer from respiratory distress, fail to turn pink, and die within 20 minutes (Yadav et al., 2003). Western blot analysis of lung protein (Fig. 3A) confirmed the loss of CARM1 in

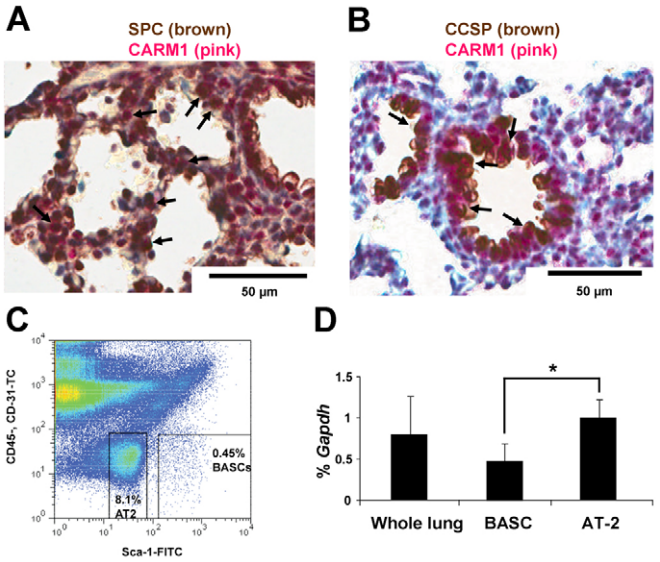


**Fig. 2. CARM1 is expressed in purified AT2 and BASC populations.** (**A**,**B**) Double staining of CARM1 (pink) with SPC or CCSP (brown) in lung sections from E18.5 mice. Arrows identify cells expressing both CARM1 and SPC or CCSP. (**C**) Representative flow cytometric profile of AT2 and bronchioalveolar stem cells (BASCs) in lungs of 12-week-old wild-type mice stained with anti-CD45 (PTPRC) conjugated to tri-color (TC), anti-CD31-TC (pecam1), and anti-Sca-1 (LY6A) conjugated to FITC. AT2 cells are $CD45^{-}$ $CD31^{-}$ with high autofluorescence in the FITC channel and 8.1% of cells from whole lung are stained as AT2 (Kim et al., 2005). BASCs were identified as $Sca\text{-}1^{+}$ $CD45^{-}$ $CD31^{-}$. (**D**) qRT-PCR analysis for *Carm1* expression was performed on whole lung tissue or isolated AT2 cells from five animals and the expression relative to *Gapdh* was averaged. *, $P<0.05$, based on a two-tailed Student's *t*-test for samples of unequal variance.

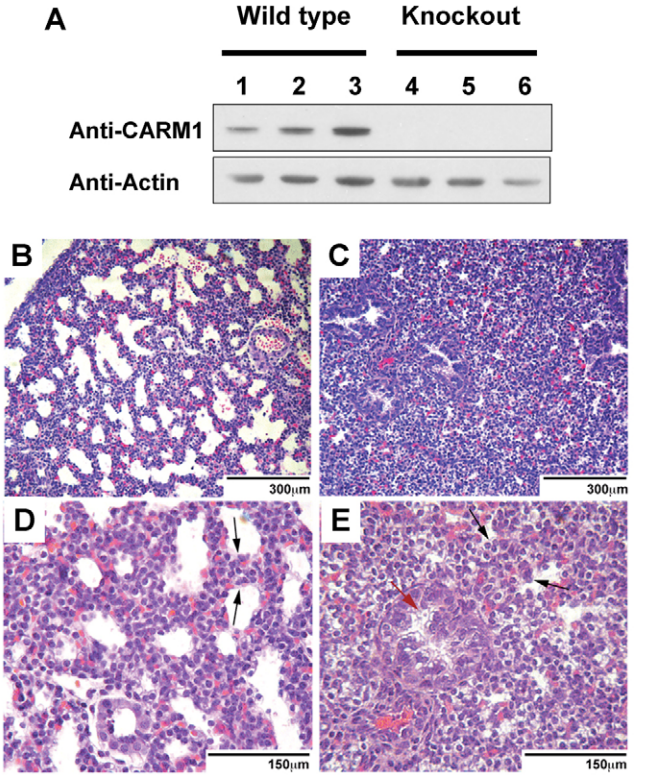


**Fig. 3. Loss of CARM1 disrupts development of the distal lung.** (**A**) Whole lung homogenates were prepared at E18.5 from wild-type (lanes 1-3) or $Carm1^{\Delta/\Delta}$ (lanes 4-6) mice and 25 μg of protein immunoblotted with polyclonal anti-CARM1. (**B-E**) Hematoxylin and Eosin (HE) staining of fixed lung tissue from wild-type (B,D) or $Carm1^{\Delta/\Delta}$ (C,E) E18.5 lungs. Severe hypercellularity, thickening of the alveolar walls (black arrows), reduced air space, and dysmorphic cells (black arrows) are observed in $Carm1^{\Delta/\Delta}$ lungs as compared with the wild type. The red arrow marks the presence of a terminal bronchiole in the $Carm1^{\Delta/\Delta}$ lungs.

the lungs of $Carm1^{\Delta/\Delta}$ mice (Fig. 1C). Fixed lungs stained with Hematoxylin and Eosin showed that lungs from wild-type embryos (E18.5) have alveolar sacs with air space and visible terminal bronchioles (Fig. 3B). By contrast, $Carm1^{\Delta/\Delta}$ lungs contained terminal bronchioles but had reduced air space compared with their wild-type littermates (Fig. 3C). It appears that the reduction in air space is a result of hypercellularity in the lung, rather than collapsed alveoli. Closer examination revealed that, whereas the airspace of wild-type lungs is lined by flat epithelial cells (Fig. 3D, arrows), the limited airspace in $Carm1^{\Delta/\Delta}$ lungs is lined by abnormal cuboidal cells (Fig. 3E, arrows).

Next, we asked whether the increased cellularity was a result of active proliferation of pulmonary cells. Lung tissue from wild-type and $Carm1^{\Delta/\Delta}$ E18.5 lungs was stained with antibody against Ki-67 (Mki67 – Mouse Genome Informatics), a nuclear antigen expressed in actively dividing cells. As expected, we observed some positive staining for Ki-67 in wild-type lung, reflecting the late stage of embryonic development of this tissue (Fig. 4A). By comparison, we saw a striking increase in the amount of Ki-67 staining in the $Carm1^{\Delta/\Delta}$ lung (Fig. 4B). These data demonstrate that in the lung, loss of CARM1 results in increased cellular proliferation, in contrast to observations made in breast and prostate in which loss of CARM1 inhibits proliferation.

Given that we observed CARM1 expression in AT2 cells (Fig. 2A,D), we asked whether the rapidly dividing cells were of AT2 origin. We stained $Carm1^{\Delta/\Delta}$ lungs for SPC (Fig. 4C, brown) and Ki-67 (Fig. 4C, pink). We observed substantial overlap, indicating that Ki-67 is expressed in some SPC-positive AT2 cells (Fig. 4C, thick arrows). Interestingly, we also detected SPC-negative Ki-67-positive cells (Fig. 4B, thin arrows). It is possible that these cells are immature AT2 cells that are actively dividing but have not yet produced SPC.

The hypercellularity observed in the absence of CARM1 might result from decreased apoptosis in addition to active proliferation. To determine whether apoptosis is up- or downregulated in the absence of CARM1, we performed TUNEL staining on fixed lung tissue from E18.5 lungs of five wild-type and five $Carm1^{\Delta/\Delta}$ animals. We counted the number of positively staining cells per field in each specimen and observed a modest 30% decrease in apoptosis in $Carm1^{\Delta/\Delta}$ lungs compared with the wild type. This reduction was statistically insignificant ($P$=0.2; data not shown), due in part to the low number of cells that were stained in the wild-type and $Carm1^{\Delta/\Delta}$ lungs. These data suggested that the hypercellularity in the $Carm1^{\Delta/\Delta}$ lung is primarily a result of cellular proliferation rather than a loss of apoptosis.

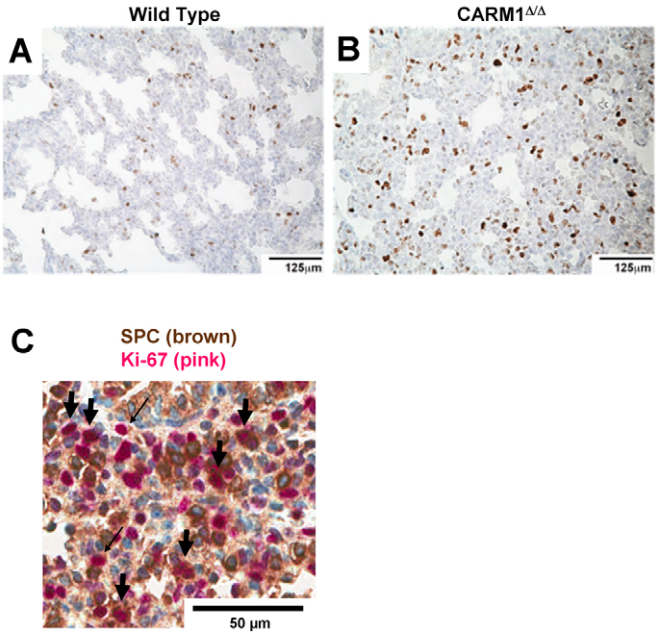


**Fig. 4. Increased proliferation of pulmonary cells in the absence of CARM1.** (**A**,**B**) Wild-type (A) and *Carm1*$^{\Delta/\Delta}$ (B) E18.5 mouse lungs were fixed and stained for Ki-67, a marker of cell division. Increased Ki-67 staining is observed in *Carm1*$^{\Delta/\Delta}$ lungs as compared with the wild type. (**C**) Double staining of Ki-67 (pink) and SPC (brown) in lung sections from E18.5 *Carm1*$^{\Delta/\Delta}$ mice. Thick arrows identify cells expressing both Ki-67 and SPC. Thin arrows identify cells expressing Ki-67 but not SPC.

## CARM1 is required for differentiation of AT2 cells

Next, we sought to gauge the level of cellular differentiation in *Carm1* knockout lungs. During pulmonary development, cytoplasmic glycogen is abundant in immature AT2 cells and decreases as it is utilized to produce surfactant protein that accumulates in the cytoplasm in the form of lamellar bodies that are then secreted into the alveolar space. In addition to their role in producing surfactant, AT2 cells serve as the precursors of AT1 epithelial cells that are required for gas exchange in the distal lung. We used transmission electron microscopy (TEM) to determine the level of cellular differentiation in wild-type and *Carm1*$^{\Delta/\Delta}$ lungs. At E18.5, AT2 cells in wild-type lungs contain some glycogen and visible lamellar bodies. Furthermore, the pulmonary air space is lined by a flat layer of AT1 cells (Fig. 5A). In *Carm1*$^{\Delta/\Delta}$ lungs, AT2 cells contained abundant glycogen in the cytoplasm, consistent with incomplete cellular maturation, and lamellar bodies. Although the presence of lamellar bodies and the production of some surfactant suggest a degree of maturation of AT2 cells in the absence of CARM1, we did not observe any AT1 cells in TEM images of lungs from *Carm1*$^{\Delta/\Delta}$ embryos after analyzing three knockout embryonic lungs alongside three lungs from wild-type littermates (Fig. 5B).

To verify the striking loss of AT1 cells in *Carm1*$^{\Delta/\Delta}$ lungs, we performed IHC with antibody against aquaporin 5 (AQP5), a water channel protein that is expressed in, and required for, the function of AT1 cells (Verkman et al., 2000). We observed AQP5 staining throughout wild-type lung (Fig. 5C,E). As expected, staining was restricted to cells lining the air space, consistent with the role of AQP5 in the function of AT1 cells. In the knockout lung, AQP5

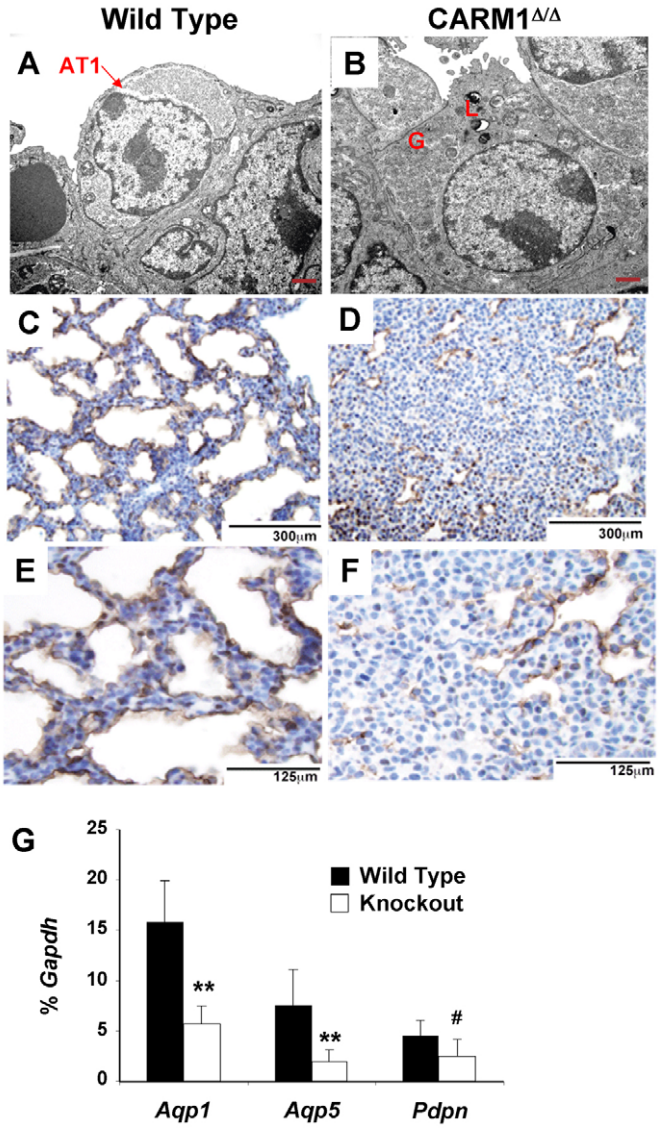


**Fig. 5. CARM1 is required for differentiation to AT1 cells in the developing lung.** (**A**,**B**) Lungs from wild-type (A) and *Carm1*$^{\Delta/\Delta}$ (B) E18.5 mice were fixed and processed for TEM (see Materials and methods). (A) Lamellar bodies, small patches of cytoplasmic glycogen and AT1 cells are visible in wild-type lung. By contrast, *Carm1*$^{\Delta/\Delta}$ lungs (B) contain an overabundance of glycogen (G) and visible lamellar bodies (L), but no AT1 cells. The presence of lamellar bodies indicates some AT2 development that is blocked before differentiation to AT1 cells. Scale bars: 1 μm. (**C-F**) IHC of lungs from wild-type (C,E) and *Carm1*$^{\Delta/\Delta}$ (D,F) E18.5 mice with anti-AQP5 shows reduced staining and abnormal morphology of AT1 cells in *Carm1*$^{\Delta/\Delta}$ lungs. (**G**) qRT-PCR analysis of markers of AT1 cells indicates loss of this cell type in *Carm1*$^{\Delta/\Delta}$ lungs. qRT-PCR was performed using RNA isolated from five wild-type and five *Carm1*$^{\Delta/\Delta}$ E18.5 lungs. Mean and s.d. are expressed as a percentage of *Gapdh* expression. **, $P<0.01$; #, $P=0.075$.

expression was observed in an aberrant pattern and was substantially reduced (Fig. 5D,F). Many AQP5 positively stained cells were rounded, misshapen and within regions of high cellularity. In addition, some of the air spaces in the *Carm1*$^{\Delta/\Delta}$ lungs lacked AQP5-positive cells altogether. These observations indicated a severe depletion of AT1 cells, consistent with observations made by TEM.

In addition to morphological analysis, we performed qRT-PCR analysis to measure genes expressed by AT1 cells. We observed a 64% and 75% ($P$<0.005) loss of *Aqp1* and *Aqp5*, respectively, in *Carm1*$^{\Delta/\Delta}$ lung compared with the wild type (Fig. 5G). We also observed a 45% decrease ($P$=0.075, Fig. 5G) in *Pdpn* (*T1*$\alpha$), which encodes an apical membrane protein that is expressed in AT1 cells and is required for their differentiation (Ramirez et al., 2003). Taken together, these data suggest that CARM1 functions in the terminal differentiation of AT2 and in the appearance of AT1 cells during embryonic development.

We hypothesized that the increased cellularity in the absence of CARM1 might consist of immature AT2 cells. We stained fixed lung from *Carm1*$^{\Delta/\Delta}$ embryos with antibody against SPC, a marker of AT2 cells (Glasser et al., 1991). SPC staining occurred throughout the wild-type lung as expected (Fig. 6A), but was substantially higher in the *Carm1*$^{\Delta/\Delta}$ lung (Fig. 6B). In addition, we observed SPC staining in cells lining terminal bronchioles in the *Carm1*$^{\Delta/\Delta}$ lung, where SPC is not normally expressed (compare Fig. 6B with 6A). By contrast, we observed similar staining of CCSP in cells surrounding the terminal bronchioles in wild-type and *Carm1*$^{\Delta/\Delta}$ lungs (Fig. 6C,D).

We next assessed whether *Carm1*$^{\Delta/\Delta}$ AT2 cells produce other members of the surfactant protein family. We used qRT-PCR to measure the expression of the genes encoding surfactant proteins SPA (*Sftpa1*), SPB (*Sftpb*) and SPD (*Sftpd*). We observed a 53% decrease in *Sftpa1* in *Carm1*$^{\Delta/\Delta}$ lungs compared with the wild type, but no decrease in *Sftpb* or *Sftpd* (Fig. 6E). The increased glycogen observed by TEM, the increased staining of SPC throughout the lung, and these data showing decreased *Sftpa1*, suggest that the *Carm1*$^{\Delta/\Delta}$ AT2 cells might not function normally for surfactant production. Interestingly, despite the fact that we observed an increased distribution of SPC protein by IHC, we observed no significant difference in SPC transcript (*Sftpc*) expression in *Carm1*$^{\Delta/\Delta}$ versus wild-type lungs (Fig. 6E). Given that IHC is not quantitative, it is possible that SPC is expressed by more cells but at a quantitatively lower level. Alternatively, the protein might not be secreted or degraded properly and accumulates in the cytoplasm. Taken together, these results reveal that loss of CARM1 results in hyperproliferation of AT2 cells and blocks their differentiation to AT1 cells.

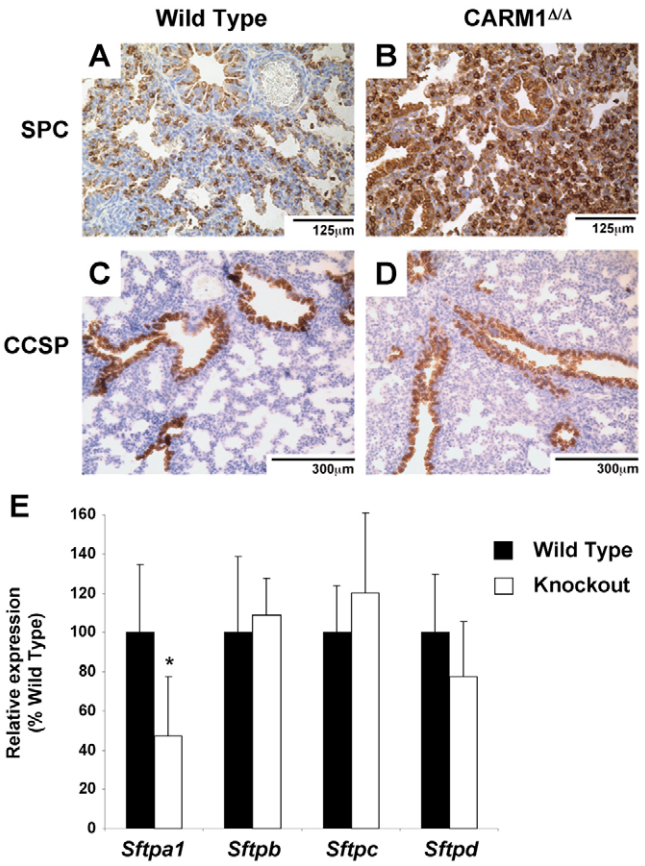


**Fig. 6. Altered AT2 differentiation in the absence of CARM1.** (**A-D**) Immunohistochemical analysis of fixed lung tissue from E18.5 wild-type (A,C) or *Carm1*$^{\Delta/\Delta}$ (B,D) mice. (A,B) Increased staining by anti-SPC in *Carm1*$^{\Delta/\Delta}$ lungs demonstrates that the increased cellularity is of AT2 origin. (C,D) Staining of CCSP, a marker of Clara epithelial cells, reveals no difference in cellular distribution. (**E**) qRT-PCR analysis of surfactant protein (*Sftpa1*, *Sftpb*, *Sftpc* and *Sftpd*) expression was performed using RNA isolated from five wild-type and five *Carm1*$^{\Delta/\Delta}$ E18.5 lungs. Mean and s.d. are expressed as a percentage of *Gapdh* expression. *, $P$<0.05.

## Loss of CARM1 disrupts glucocorticoid-mediated transcriptional regulation in pulmonary cells

To identify how CARM1 might regulate pulmonary cell growth, we compared mRNA expression profiles in lungs from E18.5 *Carm1*$^{\Delta/\Delta}$ mice and wild-type littermates. To reduce false positives, transcripts that were absent or had expression values below 40 in all samples were removed from further analysis. Comparison of E18.5 *Carm1*$^{\Delta/\Delta}$ mice and wild-type littermates identified 847 differentially expressed transcripts (LCB>1.2 and FC>1.5; see Table S2 in the supplementary material). Consistent with our previous qRT-PCR data, microarray analysis (GEO accession number GSE21606) revealed a loss of markers of AT1 cells, including *Aqp1* and *Aqp5* (Fig. 5G; see Table S2 in the supplementary material).

We performed canonical pathway-based enrichment analysis to identify which pathways and cellular functions were most disrupted by the loss of CARM1. The results suggested defects in metaphase checkpoint, cell cycle regulation and replication of DNA during cell division (Fig. 7A), consistent with the observed hyperproliferation of alveolar cells. For validation, we performed qRT-PCR analysis of eight genes identified in the microarray expression profile (see Table S2 in the supplementary material). The cell cycle inhibitor downstream of p53, *Gadd45g*, the pro-apoptotic gene *Scn3b* (Adachi et al., 2004), and the negative regulator of the WNT pathway, *Nkd1*, were significantly decreased in *Carm1*$^{\Delta/\Delta}$ lungs ($P$<0.01; Fig. 7B). We also detected an increasing trend in *Cpa3* and *Cdc6*, although the values were not significant ($P$=0.05 and 0.07, respectively; Fig. 7B). Reduced expression of p53 target genes (*Gadd45g* and Scn3b) is consistent with a previous report demonstrating that CARM1 serves as a coactivator for *p53* transcription (An et al., 2004). Indeed, we did not observe increased *p53* in the array (see Table S2 in the supplementary material).

It has been demonstrated that steroids play a central role in lung development and morphogenesis, including alveolar differentiation and surfactant production (Cole et al., 1995; Malpel et al., 2000). Interestingly, the phenotypes of glucocorticoid receptor (*Nr3c1* – Mouse Genome Informatics) knockout (*GR*$^{\Delta/\Delta}$) and *Carm1*$^{\Delta/\Delta}$ lungs are strikingly similar. Both knockout animals die shortly after birth and suffer from respiratory distress. In addition, both knockout animals have increased proliferation of AT2 cells as measured by

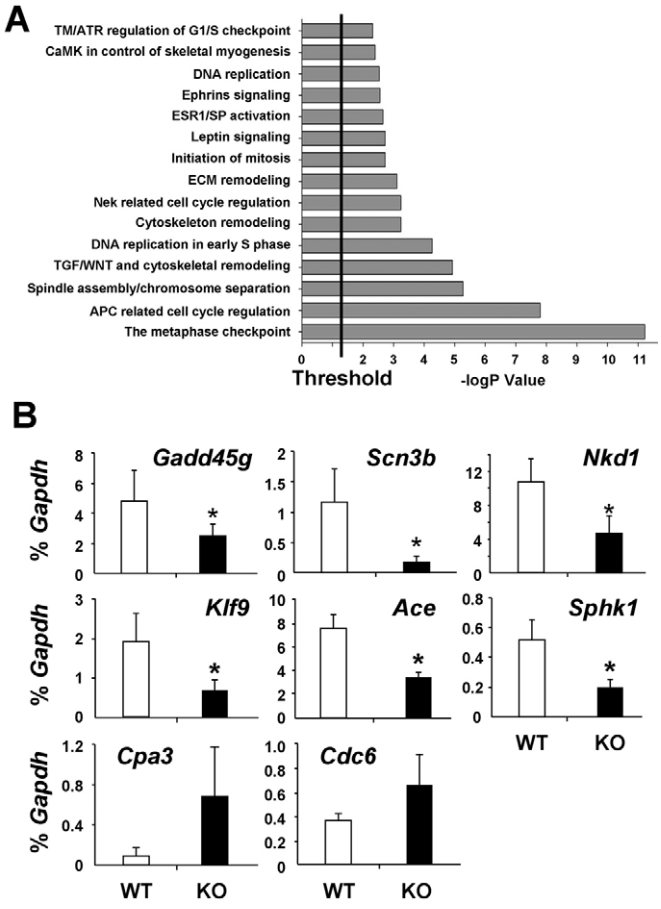


**Fig. 7. Gene expression analysis reveals dysregulation of cell cycle-related genes in *Carm1*$^{\Delta/\Delta}$ lungs.** (**A**) Gene expression analysis demonstrates increases in pathways regulating the metaphase checkpoint, the cell cycle, cellular division and cytoskeletal remodeling. (**B**) qRT-PCR analysis validates the microarray results, showing decreased expression of *Gadd45g*, *Scn3b*, *Nkd1*, *Klf9*, *Ace*, and *Sphk1*, and increased expression of *Cpa3* and *Cdc6*. Mean and s.d. are expressed as a percentage of *Gapdh* expression. *, $P$<0.05.

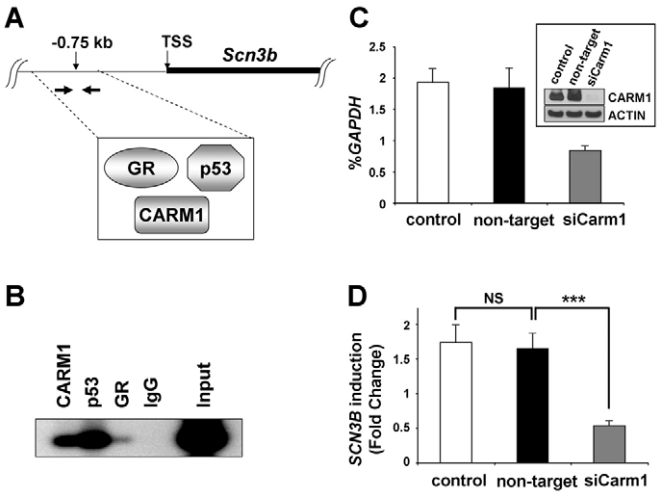


**Fig. 8. CARM1, GR and p53 interact with the proximal promoter of the *Scn3b* gene.** (**A**) Putative p53 and glucocorticoid receptor (GR) binding sites in the proximal promoter of *Scn3b*, shown forming a complex with CARM1. Horizontal arrows indicate the positions of the primers used in PCR in the ChIP assays. (**B**) ChIP assay (Southern blot shown) demonstrating binding of GR and p53 to the proximal promoter of *Scn3b* (gi:149259969) in lung cell isolates from wild-type mice. Note that CARM1 immunoprecipitation detects *Scn3b*, suggesting that a complex forms between CARM1, p53 and GR. (**C**) Knockdown of CARM1 by siRNA. Human BEAS-2B cells were transfected with *Carm1* siRNA (siCarm1), non-target siRNA (non-target), or left untransfected (control) for 48 hours. RNA was isolated and expression of *Carm1* analyzed by qRT-PCR. Error bars indicate s.d. ($n$=5). (Inset) Expression of CARM1 as detected by western blot analysis. (**D**) Upregulation of *SCN3B* is suppressed by CARM1 knockdown. BEAS-2B cells transfected with siRNAs were incubated in the presence of ethanol (vehicle control) or 500 nM dexamethasone for 72 hours. RNA was isolated and expression of *SCN3B* mRNA was analyzed by qRT-PCR. The fold change in *SCN3B* expression was calculated by comparing dexamethasone-treated and vehicle control-treated cells. Error bars indicate s.d. ($n$=5). ***, $P$ <0.001; NS, not significant.

Ki-67 IHC and display a block in differentiation of AT2 cells, with increased cytoplasmic glycogen while still producing lamellar bodies and expressing some surfactant proteins (Bird et al., 2007; Cole et al., 2004). Previous reports show that CARM1 functions as a coactivator for steroid receptor transcription, including GR activity (Chen et al., 2000). Therefore, we hypothesized that CARM1 could be regulating *GR* transcriptional activity in the lung. We first examined whether CARM1 regulates expression of *GR*, such that loss of GR might account for the phenotype observed in the *Carm1*$^{\Delta/\Delta}$ lung. However, we did not see any changes in *GR* (*Nr3c1*) mRNA expression by microarray or qRT-PCR (see Fig. S2 in the supplementary material).

Recently, gene expression analysis was performed on whole lung tissue from E18.5 wild-type and *GR*$^{\Delta/\Delta}$ lungs (Bird et al., 2007). To determine whether CARM1 and GR regulate similar patterns of gene expression, we performed a comparative analysis of the gene expression arrays from *GR*$^{\Delta/\Delta}$ and *Carm1*$^{\Delta/\Delta}$ lungs (see Table S3 in the supplementary material). A significant overlap ($P$<0.05) of 154 genes was identified between *GR*$^{\Delta/\Delta}$ and *Carm1*$^{\Delta/\Delta}$ differentially expressed genes (see Table S3 in the supplementary material). The overlapping genes account for more than 22% of all genes identified in the *Carm1*$^{\Delta/\Delta}$ expression profile, and include *Gadd45g*, *Scn3b*, *Nkd1*, *Klf9*, *Ace*, *Sphk1* and *Cdc6* (Fig. 7B).

Next, we investigated whether CARM1 cooperates with GR to induce target genes in vivo. We investigated *Scn3b*, which is induced by DNA damage in a p53-dependent manner (Adachi et al., 2004) and is substantially downregulated in both *Carm1*$^{\Delta/\Delta}$ and *GR*$^{\Delta/\Delta}$ lungs. In addition to a p53 binding site, we identified a GR binding site in the promoter region of *Scn3b*. We designed primers to amplify the fragment containing the binding sites for p53 and GR (Fig. 8A), and performed a chromatin immunoprecipitation (ChIP) assay. As shown in Fig. 8B, both p53 and GR bound to the promoter region. The strong band was also detected in CARM1 antibody-treated extracts, suggesting that CARM1 forms a complex with p53 and/or GR and mediates their transcriptional activity.

Finally, we sought to determine whether knockdown of CARM1 perturbs glucocorticoid activity in bronchial epithelial cells. To this end, we used BEAS-2B cells, a human immortalized bronchial epithelial cell line. Cells transiently transfected with siRNA against

*Carm1* showed substantially reduced CARM1 expression at both the mRNA and protein levels, in comparison to cells transfected with non-targeting siRNA or non-transfected control cells (Fig. 8C). Next, we examined whether glucocorticoid (dexamethasone) upregulates *SCN3B* expression in BEAS-2B cells. In dexamethasone-treated control cells or those transfected with non-targeting siRNA, *SCN3B* expression increased by 1.7±0.25-fold or 1.6±0.22-fold, respectively, compared with vehicle-treated cells. However, *SCN3B* expression was downregulated with dexamethasone treatment in CARM1 knockdown cells (0.5±0.07-fold; Fig. 8D), suggesting not only that CARM1 is required for induction of *SCN3B* upon glucocorticoid stimulation, but also that glucocorticoid might negatively regulate *SCN3B* expression in the absence of CARM1. By contrast, dexamethasone treatment upregulated *CDC6* in CARM1 knockdown cells, whereas the treatment had a minimal effect on *CDC6* expression in control cells (2.0±0.2-fold; see Fig. S3 in the supplementary material). These results are consistent with our observation that *Cdc6* was upregulated in $Carm1^{\Delta/\Delta}$ mouse lung, and indicate that CARM1 may suppress *CDC6* upregulation induced by dexamethasone (Fig. 7B).

Taken together, these data suggest that CARM1 and GR regulate a similar array of genes in embryonic lung, and that the effects of glucocorticoid hormone on gene transcription are at least in part dependent on CARM1.

## DISCUSSION

The results of this study demonstrate a crucial role for CARM1 in pulmonary development. We show CARM1 expression in airway and alveolar epithelial cells, BASCs and endothelial cells. We demonstrate that AT2 cells fail to complete differentiation and hyperproliferate in the absence of CARM1. We also show a block in AT1 cell differentiation in $Carm1^{\Delta/\Delta}$ lungs. Lastly, gene expression analysis reveals a dysregulation of genes that regulate the cell cycle and proliferation, and a striking overlap between CARM1 and GR gene expression signatures, indicating that loss of CARM1 disrupts GR signaling.

The finding that AT2 cells hyperproliferate in the absence of CARM1 had not been anticipated, given that CARM1 expression is increased in breast and prostate tumors, and knockdown of CARM1 in these cell types results in decreased proliferation in response to hormone stimulation (El Messaoudi et al., 2006; Frietze et al., 2008; Hong et al., 2004; Majumder et al., 2006). In these studies, CARM1 was shown to positively regulate cyclin E1 and E2F1, and it was hypothesized that loss of these factors contributes to the loss of proliferation in the CARM1 knockdown cells. We did not see changes in the expression of these factors in our gene expression analysis or in qRT-PCR of RNA from $Carm1^{\Delta/\Delta}$ lungs (see Fig. S2 in the supplementary material). These results suggest that the role of CARM1 is cell-type specific.

The overlap in gene expression in the $Carm1^{\Delta/\Delta}$ lung and $GR^{\Delta/\Delta}$ lung is striking. Eleven out of 23 genes that we identified as regulating the cell cycle, cell proliferation and apoptosis in the $Carm1^{\Delta/\Delta}$ lung are also dysregulated in $GR^{\Delta/\Delta}$ lungs. These data support the hypothesis that, at least in part, CARM1 functions with GR to regulate the expression of genes that regulate cellular proliferation and are consistent with previous reports that CARM1 functions as a coactivator of *GR* transcription. CARM1 has been shown to bind glucocorticoid-interacting protein (GRIP1) and to synergistically function to increase *GR* transcriptional activity in response to the synthetic corticosteroid, dexamethasone (Lee et al., 2005; Liu et al., 2006; Teyssier et al., 2006). Consistent with these reports, we demonstrated that knockdown of CARM1 disrupts changes in gene expression induced by dexamethasone in bronchial epithelial cells (Fig. 8D; see Fig. S3 in the supplementary material).

Although the lung phenotypes of $Carm1^{\Delta/\Delta}$ and $GR^{\Delta/\Delta}$ are similar, CARM1 is likely to function in additional capacities during lung development, other than solely as a coactivator for GR. Although the overlap in dysregulated genes observed in the expression arrays is substantial, it represents only a fraction of the genes dysregulated in each of the knockout animals. Several other mouse models display similar phenotypes to $Carm1^{\Delta/\Delta}$ animals. Loss of the transcription factor C/EBPα results in hyperproliferation of AT2 cells, a block in AT2 differentiation and loss of AT1 cells (Basseres et al., 2006; Martis et al., 2006). In the case of C/EBPα, the block in AT2 differentiation is earlier than for CARM1, with no lamellar bodies and more substantial loss of surfactant proteins. We performed western blot analysis and qRT-PCR and observed no loss of C/EBPα in $Carm1^{\Delta/\Delta}$ lungs (data not shown). Similarly, gene expression profiling reveals no loss of *Carm1* expression in lungs with a targeted deletion of *Cebpa* in SPC-producing pulmonary cells (Basseres et al., 2006). In addition, qRT-PCR of RNA from $Carm1^{\Delta/\Delta}$ lungs shows normal expression of *Foxa2* (*Hnf3*β), a transcriptional target of C/EBPα, the loss of which results in a similar phenotype to *Cebpa* knockouts (Halmos et al., 2004; Wan et al., 2004). Overexpression of NOTCH3 also leads to a block in AT2 and AT1 differentiation, although without hyperproliferation of AT2 cells (Dang et al., 2003), and loss of KLF5 results in a similar phenotype (Wan et al., 2008). Targeted deletion of *Pdpn* is also perinatal lethal, with loss of AT1 cells and hyperproliferation of alveolar epithelial cells at a later developmental stage than for $Carm1^{\Delta/\Delta}$ lungs (perinatal) (Ramirez et al., 2003). Loss of *Pdpn* in $Carm1^{\Delta/\Delta}$ lungs is likely to contribute to the block in AT1 differentiation. However, given that CARM1 methylates histones as well as transcriptional regulators, further study will be required to determine which genes are directly regulated by CARM1 and whether this regulation is through histone methylation or interactions with transcription factors such as C/EBPα and FOXA2.

Notably, several of the factors, the loss of which in development leads to hyperproliferation of alveolar cells, are also downregulated in lung cancer. C/EBPα and FOXA2 are downregulated in lung cancer and function as tumor suppressors (Halmos et al., 2004; Halmos et al., 2002; Tada et al., 2006). Thus, this phenotype might be predictive of tumorigenesis resulting from loss of function in adulthood. As such, loss of CARM1 expression might lead to increased cell growth and tumor formation. This hypothesis is particularly attractive given that CARM1 is expressed in the BASC population. Indeed, loss of growth regulation in BASCs has been shown to contribute to tumorigenesis in several animal models (Dave et al., 2008; Dovey et al., 2008; Kim et al., 2005). To test this hypothesis, one would ideally first determine whether the BASC population exists in the absence of CARM1. However, we were unable to isolate BASCs by FACS from $Carm1^{\Delta/\Delta}$ or wild-type embryonic lung. Indeed, the BASC population increases with age and is undetectable in embryonic lung (our unpublished observations). Given that the role of BASCs in the self-renewal of lung cells remains ambiguous (Rawlins et al., 2009), further studies will be necessary to confirm how or if CARM1 functions in lung stem cells. Other molecular models might provide explanations as to how the loss of CARM1 induces hyperproliferation of alveolar cells. It has been show that deletion of *Rac1* stimulates epidermal stem cells to exit their niche and proliferate through

regulation of c-MYC in the epidermis (Benitah et al., 2005). In this model, there is a transient hyperproliferation as detected by an increase in Ki-67 staining, followed by exhaustion of the stem cell pool and self-renewal capacity. In this scenario, deletion of *Carm1* might induce BASCs or lung stem cells to exit their niche and massively enter the AT2 compartment, leading to an apparent transient hyperproliferation of this AT2 population. To further test these hypotheses, a lung cell-specific inducible deletion of *Carm1* will be required to avoid the perinatal lethality of the standard knockout. These studies will be of particular interest given the role of CARM1 in breast and prostate cancer and will shed light into the tissue specificity of CARM1 action.

**Acknowledgements**
We thank Junyan Zhang and Keona Ryland for assistance with mouse husbandry, Daniel Brown for technical expertise in electron microscopy, Drs Carla Kim and Yoji A. Minamishima for helpful discussion, and Dr Towia Liberman, head of the Beth Israel Microarray Core Facility. These studies were supported by NIH grants 5F32HL082430 to K.B.O., R00CA126026 to S.K. and R00CA131503 to U.S., a Flight Attendant Medical Research Foundation grant to E.L., NIH DK62248 and core facilities support grant NIEHS ES07784 to M.T.B., and P50 CA90578 to D.G.T. U.S. is the Diane and Arthur B. Belfer Faculty Scholar in Cancer Research of the Albert Einstein College of Medicine. Deposited in PMC for release after 12 months.

**Competing interests statement**
The authors declare no competing financial interests.

**Supplementary material**
Supplementary material for this article is available at
http://dev.biologists.org/lookup/suppl/doi:10.1242/dev.037150/-/DC1

**References**

**Adachi, K., Toyota, M., Sasaki, Y., Yamashita, T., Ishida, S., Ohe-Toyota, M., Maruyama, R., Hinoda, Y., Saito, T., Imai, K. et al.** (2004). Identification of SCN3B as a novel p53-inducible proapoptotic gene. *Oncogene* **23**, 7791-7798.
**An, W., Kim, J. and Roeder, R. G.** (2004). Ordered cooperative functions of PRMT1, p300, and CARM1 in transcriptional activation by p53. *Cell* **117**, 735-748.
**Basseres, D. S., Levantini, E., Ji, H., Monti, S., Elf, S., Dayaram, T., Fenyus, M., Kocher, O., Golub, T., Wong, K. K. et al.** (2006). Respiratory failure due to differentiation arrest and expansion of alveolar cells following lung-specific loss of the transcription factor C/EBPalpha in mice. *Mol. Cell. Biol.* **26**, 1109-1123.
**Bauer, U. M., Daujat, S., Nielsen, S. J., Nightingale, K. and Kouzarides, T.** (2002). Methylation at arginine 17 of histone H3 is linked to gene activation. *EMBO Rep.* **3**, 39-44.
**Bedford, M. T. and Richard, S.** (2005). Arginine methylation an emerging regulator of protein function. *Mol. Cell* **18**, 263-272.
**Benitah, S. A., Frye, M., Glogauer, M. and Watt, F. M.** (2005). Stem cell depletion through epidermal deletion of Rac1. *Science* **309**, 933-935.
**Bird, A. D., Tan, K. H., Olsson, P. F., Zieba, M., Flecknoe, S. J., Liddicoat, D. R., Mollard, R., Hooper, S. B. and Cole, T. J.** (2007). Identification of glucocorticoid-regulated genes that control cell proliferation during murine respiratory development. *J. Physiol.* **585**, 187-201.
**Cardoso, W. V. and Lu, J.** (2006). Regulation of early lung morphogenesis: questions, facts and controversies. *Development* **133**, 1611-1624.
**Chen, D., Huang, S. M. and Stallcup, M. R.** (2000). Synergistic, p160 coactivator-dependent enhancement of estrogen receptor function by CARM1 and p300. *J. Biol. Chem.* **275**, 40810-40816.
**Cheng, D., Cote, J., Shaaban, S. and Bedford, M. T.** (2007). The arginine methyltransferase CARM1 regulates the coupling of transcription and mRNA processing. *Mol. Cell* **25**, 71-83.
**Chevillard-Briet, M., Trouche, D. and Vandel, L.** (2002). Control of CBP co-activating activity by arginine methylation. *EMBO J.* **21**, 5457-5466.
**Cole, T. J., Blendy, J. A., Monaghan, A. P., Krieglstein, K., Schmid, W., Aguzzi, A., Fantuzzi, G., Hummler, E., Unsicker, K. and Schutz, G.** (1995). Targeted disruption of the glucocorticoid receptor gene blocks adrenergic chromaffin cell development and severely retards lung maturation. *Genes Dev.* **9**, 1608-1621.
**Cole, T. J., Solomon, N. M., Van Driel, R., Monk, J. A., Bird, D., Richardson, S. J., Dilley, R. J. and Hooper, S. B.** (2004). Altered epithelial cell proportions in the fetal lung of glucocorticoid receptor null mice. *Am. J. Respir. Cell Mol. Biol.* **30**, 613-619.
**Cook, J. R., Lee, J. H., Yang, Z. H., Krause, C. D., Herth, N., Hoffmann, R. and Pestka, S.** (2006). FBXO11/PRMT9, a new protein arginine methyltransferase, symmetrically dimethylates arginine residues. *Biochem. Biophys. Res. Commun.* **342**, 472-481.
**Covic, M., Hassa, P. O., Saccani, S., Buerki, C., Meier, N. I., Lombardi, C., Imhof, R., Bedford, M. T., Natoli, G. and Hottiger, M. O.** (2005). Arginine methyltransferase CARM1 is a promoter-specific regulator of NF-kappaB-dependent gene expression. *EMBO J.* **24**, 85-96.
**Dang, T. P., Eichenberger, S., Gonzalez, A., Olson, S. and Carbone, D. P.** (2003). Constitutive activation of Notch3 inhibits terminal epithelial differentiation in lungs of transgenic mice. *Oncogene* **22**, 1988-1997.
**Daujat, S., Bauer, U. M., Shah, V., Turner, B., Berger, S. and Kouzarides, T.** (2002). Crosstalk between CARM1 methylation and CBP acetylation on histone H3. *Curr. Biol.* **12**, 2090-2097.
**Dave, V., Wert, S. E., Tanner, T., Thitoff, A. R., Loudy, D. E. and Whitsett, J. A.** (2008). Conditional deletion of Pten causes bronchiolar hyperplasia. *Am. J. Respir. Cell Mol. Biol.* **38**, 337-345.
**Dovey, J. S., Zacharek, S. J., Kim, C. F. and Lees, J. A.** (2008). Bmi1 is critical for lung tumorigenesis and bronchioalveolar stem cell expansion. *Proc. Natl. Acad. Sci. USA* **105**, 11857-11862.
**Ebralidze, A. K., Guibal, F. C., Steidl, U., Zhang, P., Lee, S., Bartholdy, B., Jorda, M. A., Petkova, V., Rosenbauer, F., Huang, G. et al.** (2008). PU.1 expression is modulated by the balance of functional sense and antisense RNAs regulated by a shared cis-regulatory element. *Genes Dev.* **22**, 2085-2092.
**El Messaoudi, S., Fabbrizio, E., Rodriguez, C., Chuchana, P., Fauquier, L., Cheng, D., Theillet, C., Vandel, L., Bedford, M. T. and Sardet, C.** (2006). Coactivator-associated arginine methyltransferase 1 (CARM1) is a positive regulator of the Cyclin E1 gene. *Proc. Natl. Acad. Sci. USA* **103**, 13351-13356.
**Fauquier, L., Duboe, C., Jore, C., Trouche, D. and Vandel, L.** (2008). Dual role of the arginine methyltransferase CARM1 in the regulation of c-Fos target genes. *FASEB J.* **22**, 3337-3347
**Feng, Q., Yi, P., Wong, J. and O'Malley, B. W.** (2006). Signaling within a coactivator complex: methylation of SRC-3/AIB1 is a molecular switch for complex disassembly. *Mol. Cell. Biol.* **26**, 7846-7857.
**Frietze, S., Lupien, M., Silver, P. A. and Brown, M.** (2008). CARM1 regulates estrogen-stimulated breast cancer growth through up-regulation of E2F1. *Cancer Res.* **68**, 301-306.
**Fujiwara, T., Mori, Y., Chu, D. L., Koyama, Y., Miyata, S., Tanaka, H., Yachi, K., Kubo, T., Yoshikawa, H. and Tohyama, M.** (2006). CARM1 regulates proliferation of PC12 cells by methylating HuD. *Mol. Cell. Biol.* **26**, 2273-2285.
**Glasser, S. W., Korfhagen, T. R., Wert, S. E., Bruno, M. D., McWilliams, K. M., Vorbroker, D. K. and Whitsett, J. A.** (1991). Genetic element from human surfactant protein SP-C gene confers bronchiolar-alveolar cell specificity in transgenic mice. *Am. J. Physiol.* **261**, L349-L356.
**Halmos, B., Huettner, C. S., Kocher, O., Ferenczi, K., Karp, D. D. and Tenen, D. G.** (2002). Down-regulation and antiproliferative role of C/EBPalpha in lung cancer. *Cancer Res.* **62**, 528-534.
**Halmos, B., Basseres, D. S., Monti, S., D'Alo, F., Dayaram, T., Ferenczi, K., Wouters, B. J., Huettner, C. S., Golub, T. R. and Tenen, D. G.** (2004). A transcriptional profiling study of CCAAT/enhancer binding protein targets identifies hepatocyte nuclear factor 3 beta as a novel tumor suppressor in lung cancer. *Cancer Res.* **64**, 4137-4147.
**Hong, H., Kao, C., Jeng, M. H., Eble, J. N., Koch, M. O., Gardner, T. A., Zhang, S., Li, L., Pan, C. X., Hu, Z. et al.** (2004). Aberrant expression of CARM1, a transcriptional coactivator of androgen receptor, in the development of prostate carcinoma and androgen-independent status. *Cancer* **101**, 83-89.
**Kim, C. F., Jackson, E. L., Woolfenden, A. E., Lawrence, S., Babar, I., Vogel, S., Crowley, D., Bronson, R. T. and Jacks, T.** (2005). Identification of bronchioalveolar stem cells in normal lung and lung cancer. *Cell* **121**, 823-835.
**Kim, D., Lee, J., Cheng, D., Li, J., Carter, C., Richie, E. and Bedford, M. T.** (2009). Enzymatic activity is required for the in vivo functions of the coactivator-associated arginine methyltransferase 1. *J. Biol. Chem.* **285**, 1147-1152.
**Kim, J., Lee, J., Yadav, N., Wu, Q., Carter, C., Richard, S., Richie, E. and Bedford, M. T.** (2004). Loss of CARM1 results in hypomethylation of thymocyte cyclic AMP-regulated phosphoprotein and deregulated early T cell development. *J. Biol. Chem.* **279**, 25339-25344.
**Koh, S. S., Li, H., Lee, Y. H., Widelitz, R. B., Chuong, C. M. and Stallcup, M. R.** (2002). Synergistic coactivator function by coactivator-associated arginine methyltransferase (CARM) 1 and beta-catenin with two different classes of DNA-binding transcriptional activators. *J. Biol. Chem.* **277**, 26031-26035.
**Lee, D. Y., Teyssier, C., Strahl, B. D. and Stallcup, M. R.** (2005). Role of protein methylation in regulation of transcription. *Endocr. Rev.* **26**, 147-170.
**Li, H., Park, S., Kilburn, B., Jelinek, M. A., Henschen-Edman, A., Aswad, D. W., Stallcup, M. R. and Laird-Offringa, I. A.** (2002). Lipopolysaccharide-induced methylation of HuR, an mRNA-stabilizing protein, by CARM1. Coactivator-associated arginine methyltransferase. *J. Biol. Chem.* **277**, 44623-44630.
**Liu, P. Y., Hsieh, T. Y., Chou, W. Y. and Huang, S. M.** (2006). Modulation of glucocorticoid receptor-interacting protein 1 (GRIP1) transactivation and co-

activation activities through its C-terminal repression and self-association domains. *FEBS J.* **273**, 2172-2183.
**Ma, H., Baumann, C. T., Li, H., Strahl, B. D., Rice, R., Jelinek, M. A., Aswad, D. W., Allis, C. D., Hager, G. L. and Stallcup, M. R.** (2001). Hormone-dependent, CARM1-directed, arginine-specific methylation of histone H3 on a steroid-regulated promoter. *Curr. Biol.* **11**, 1981-1985.
**Maeda, Y., Dave, V. and Whitsett, J. A.** (2007). Transcriptional control of lung morphogenesis. *Physiol. Rev.* **87**, 219-244.
**Majumder, S., Liu, Y., Ford, O. H., 3rd, Mohler, J. L. and Whang, Y. E.** (2006). Involvement of arginine methyltransferase CARM1 in androgen receptor function and prostate cancer cell viability. *Prostate* **66**, 1292-1301.
**Malpel, S., Mendelsohn, C. and Cardoso, W. V.** (2000). Regulation of retinoic acid signaling during lung morphogenesis. *Development* **127**, 3057-3067.
**Martis, P. C., Whitsett, J. A., Xu, Y., Perl, A. K., Wan, H. and Ikegami, M.** (2006). C/EBPalpha is required for lung maturation at birth. *Development* **133**, 1155-1164.
**Mastrianni, D. M., Eddy, R. L., Rosenberg, H. F., Corrette, S. E., Shows, T. B., Tenen, D. G. and Ackerman, S. J.** (1992). Localization of the human eosinophil Charcot-Leyden crystal protein (lysophospholipase) gene (CLC) to chromosome 19 and the human ribonuclease 2 (eosinophil-derived neurotoxin) and ribonuclease 3 (eosinophil cationic protein) genes (RNS2 and RNS3) to chromosome 14. *Genomics* **13**, 240-242.
**Miao, F., Li, S., Chavez, V., Lanting, L. and Natarajan, R.** (2006). Coactivator-associated arginine methyltransferase-1 enhances nuclear factor-kappaB-mediated gene transcription through methylation of histone H3 at arginine 17. *Mol. Endocrinol.* **20**, 1562-1573.
**Quandt, K., Frech, K., Karas, H., Wingender, E. and Werner, T.** (1995). MatInd and MatInspector: new fast and versatile tools for detection of consensus matches in nucleotide sequence data. *Nucleic Acids Res.* **23**, 4878-4884.
**Ramirez, M. I., Millien, G., Hinds, A., Cao, Y., Seldin, D. C. and Williams, M. C.** (2003). T1alpha, a lung type I cell differentiation gene, is required for normal lung cell proliferation and alveolus formation at birth. *Dev. Biol.* **256**, 61-72.
**Rawlins, E. L., Okubo, T., Xue, Y., Brass, D. M., Auten, R. L., Hasegawa, H., Wang, F. and Hogan, B. L.** (2009). The role of Scgb1a1+ Clara cells in the long-term maintenance and repair of lung airway, but not alveolar, epithelium. *Cell Stem Cell* **4**, 525-534.
**Schurter, B. T., Koh, S. S., Chen, D., Bunick, G. J., Harp, J. M., Hanson, B. L., Henschen-Edman, A., Mackay, D. R., Stallcup, M. R. and Aswad, D. W.** (2001). Methylation of histone H3 by coactivator-associated arginine methyltransferase 1. *Biochemistry* **40**, 5747-5756.
**Tada, Y., Brena, R. M., Hackanson, B., Morrison, C., Otterson, G. A. and Plass, C.** (2006). Epigenetic modulation of tumor suppressor CCAAT/enhancer binding protein alpha activity in lung cancer. *J. Natl. Cancer Inst.* **98**, 396-406.
**Teyssier, C., Ou, C. Y., Khetchoumian, K., Losson, R. and Stallcup, M. R.** (2006). Transcriptional intermediary factor 1alpha mediates physical interaction and functional synergy between the coactivator-associated arginine methyltransferase 1 and glucocorticoid receptor-interacting protein 1 nuclear receptor coactivators. *Mol. Endocrinol.* **20**, 1276-1286.
**Verkman, A. S., Matthay, M. A. and Song, Y.** (2000). Aquaporin water channels and lung physiology. *Am. J. Physiol. Lung Cell Mol. Physiol.* **278**, L867-L879.
**Wan, H., Xu, Y., Ikegami, M., Stahlman, M. T., Kaestner, K. H., Ang, S. L. and Whitsett, J. A.** (2004). Foxa2 is required for transition to air breathing at birth. *Proc. Natl. Acad. Sci. USA* **101**, 14449-14454.
**Wan, H., Luo, F., Wert, S. E., Zhang, L., Xu, Y., Ikegami, M., Maeda, Y., Bell, S. M. and Whitsett, J. A.** (2008). Kruppel-like factor 5 is required for perinatal lung morphogenesis and function. *Development* **135**, 2563-2572.
**Xu, W., Chen, H., Du, K., Asahara, H., Tini, M., Emerson, B. M., Montminy, M. and Evans, R. M.** (2001). A transcriptional switch mediated by cofactor methylation. *Science* **294**, 2507-2511.
**Yadav, N., Lee, J., Kim, J., Shen, J., Hu, M. C., Aldaz, C. M. and Bedford, M. T.** (2003). Specific protein methylation defects and gene expression perturbations in coactivator-associated arginine methyltransferase 1-deficient mice. *Proc. Natl. Acad. Sci. USA* **100**, 6464-6468.
**Yadav, N., Cheng, D., Richard, S., Morel, M., Iyer, V. R., Aldaz, C. M. and Bedford, M. T.** (2008). CARM1 promotes adipocyte differentiation by coactivating PPARgamma. *EMBO Rep.* **9**, 193-198.
**Yamaguchi, Y., Tenen, D. G. and Ackerman, S. J.** (1994). Transcriptional regulation of the human eosinophil peroxidase genes: characterization of a peroxidase promoter. *Int. Arch. Allergy Immunol.* **104**, 30-31.
**Yang, C. K., Kim, J. H., Li, H. and Stallcup, M. R.** (2006). Differential use of functional domains by coiled-coil coactivator in its synergistic coactivator function with beta-catenin or GRIP1. *J. Biol. Chem.* **281**, 3389-3397.

## Table S1. Oligonucleotides used for gene expression analysis

| Gene | Sequences (5′ to 3′) |
|---|---|
| *Ace* | ATCACAGGCCAGCCTAACATGTCA, GGGCGAGACCCACGGTGGCCACGA |
| *Aqp1* | TCCTCCCTAGTCGACAATTCACTT, ATTGAGATCATTGGCACTCTGCAGCTGGTA |
| *Aqp5* | CTCCCCAGCCTTATCCATTG, TCCTACCCAGAAGACCCATGTG |
| *Carm1* | CCTACCAGCGTGCGATCCT, TGACCACGATGCGGTCTGT |
| *Ccne1* | TCAAATGGATGGTTCCGTTCGCCA, AGGTTTGGTCATTCTGTCTCCTGC |
| *Cdc6* | GGGCGAGACCCACGGTGGCCACGA, TTGATGGGAACAGGGTGACTTTGA |
| *Cpa* | ATGCTATTAATTCCTTATGGCTAC, ACATGTTGGCTTTATCCGGGATTC |
| *E2f1* | CGATTCTGACGTGCTGCTCT, CAGCGAGGTACTGATGGTCA |
| *Gadd45g* | GAAAGCACTGCACGAACTTCTG, CGCTATGTCGCCCTCATCTT |
| *Gapdh* | CCAGCCTCGTCCCGTAGAC, GCCTTGACTGTGCCGTTGA |
| *Klf9* | CCTCCCATCTTAAAGCCCATTACA, AACTCGGTGTGACGCCGGGCATGC |
| *Nkd1* | TTCAACCATACCGATCTGCAGAGC, GGCAGCTCTGACTTCTGGGCCACC |
| *Nr3c1* | TTCCACCAATTCCTGTTGGTTCTG, ATAATGGCATCCCGAAGCTTCATC |
| *p15* | GCAGCCCTGGAAGCCGGCGCAGA, GCCCCTGCCCGGTGCAGCACGACA |
| *p21* | GAACATCTCAGGGCCGAAAA, GCGCTTGGAGTGATAGAAATCTGT |
| *p53* | TGTAGCTTCAGTTCATTGGGACCA, CGTCCATGCAGTGAGGTGATGGCA |
| *Scn3b* | CCTGCCTTCAACAGATTGCTT, CTCCCTCTTCATGCAGGAGATG |
| *Sftpa1* | AGGCAGACATCCACACAGCTT, ACTTGATGCCAGCAACAACAGT |
| *Sftpb* | ACGTCCTCTGGAAGCCTTCA, TGTCTTCTTGGAGCCACAACAG |
| *Sftpc* | CCGTGCACCTCAAACGCCTTCTCA, GCCGCTGGTAGTCATACACAACGA-3 |
| *Sftpd* | ACAGCGTCTAGAGGTTGCCTTCT, CAGCTGTCCTCCAGCCTGTT |
| *Sphk1* | AATGGAACGGCCAGACTGGGAGAC, GAATAGAGCCGCAGCCCAGAAGCA |
| *Pdpn* (*T1α*) | AGGTACAGGAGACGGCATGGT, CCAGAGGTGCCTTGCCAGTA |
| *CARM1** | TCCTGATGGCCAAGTCTGTCAAGT, AGCAACGTCAAACCAGAAAGCCAG |
| *SCN3B** | TTCTACAGGCCCGAGGGCGG, TGCCATTCCACTGCAGGCGC |
| *CDC6** | GGGTGAAGGCTGCGGGTTCC, GCCCAGACGTTTCCTGGGGC |
| *GAPDH** | CCAGGCGCCCAATACG, CCACATCGCTCAGACACCAT |

*Human.